Fast numerical solution of nonlinear nonlocal cochlear models[☆]

Daniele Bertaccini[a,*], Renata Sisto[b]

[a]*Università di Roma "Tor Vergata", Dipartimento di Matematica, viale della Ricerca Scientifica 1, 00133 Roma*
[b]*INAIL, Italian Workers' Compensation Authority, National Research Centre for Occupational Safety and Prevention, Dipartimento Igiene del Lavoro, 00040 Monte Porzio Catone, Roma.*

Abstract

A fast full second order time-step algorithm for some recently proposed nonlinear, nonlocal active models for the inner ear is analyzed here. In particular, we emphasize the properties of discretized systems and the convergence of a hybrid direct-iterative solver for its approximate solution in view of the parameters of the continuous model. We found that the proposed solver is faster than standard sparse direct solvers for all the considered discrete models.

Numerical tests confirm that the proposed techniques are crucial in order to get fast and reliable simulations.

Key words and Phrases. Cochlear Modeling; Iterative methods; Integrodifferential cochlear models.

1. Introduction

We propose a framework for fast and reliable solution of the discretized versions of inner ear models based on partial integro-differential equations.

Modeling cochlea and, more in general, the various aspects of the ear's response to multifrequency inputs, has found to help prevention of various diseases and the design of the latest hearing aids technology.

The sound processing in the *inner ear* starts from input pressure waves that reach it through the *middle ear*. In mammals, frequency discrimination and active amplification are both performed in the cochlea, a cavity filled with a liquid medium, containing a tonotopically resonant vibrating membrane, the *basilar membrane* (BM for short from here on). When the input wave is a pure tone (i.e., it is made of a single frequency), the BM motion reaches its maximum

---

[*]Corresponding author
Email addresses: `bertaccini@mat.uniroma2.it` (Daniele Bertaccini), `renata.sisto@ispesl.it` (Renata Sisto)

amplitude at a specific location, the *characteristic place* (CP for short) after a short transient, lasting a few milliseconds. The frequency corresponding to CP is called *characteristic frequency*. By mapping each frequency component of a sound input to its characteristic place, the BM acts as a frequency analyzer. It is known that the cochlear dynamics is nonlocal, and strongly nonlinear, i.e., there is a dependence of the effectiveness of the local active amplification mechanism on the BM displacement amplitude within a surrounding cochlear region. In particular, the BM shows a compressive nonlinearity, i.e., responses to low-level inputs are more sensitive and sharply tuned while the high level stimuli are less.

The basilar membrane is also the base for the sensory cells of hearing, the *hair cells*. Hair cells are the sensory receptors of both the auditory system and the vestibular system in all vertebrates. In mammals, the auditory hair cells are located within the organ of Corti on the BM. Cochlear hair cells come in two anatomically and functionally distinct types: the outer and inner hair cells (OHCs and IHCs for short, respectively). OHCs are the receptor potential triggers active vibrations of the cell body. This drives oscillations in the cells length and provide an "active" feedback amplification. OHCs do not send neural signals to the brain, but they are responsible of the nonlinear response to the above mentioned compressive nonlinear response of the BM. The amplification can be by movement of their hair bundles, or by an electrically driven motility of their cell bodies. On the other hand, the IHCs transform the sound vibrations in the fluids of the cochlea into electrical signals sent via the auditory nerve to the auditory cortex. In this research, we focus on mechanical aspects and then the OHCs will play the major role.

Under certain conditions, due to nonlinearity, responses at frequencies other than the input frequencies are generated, which are called *distortion products* (DP for short). Distortion product otoacoustic emissions (DPOAEs for short), which can be recorded in the ear canal, are generated in the cochlea in response to two primary tones of given frequencies f_1 and f_2, and sound pressure level L_1 and L_2, presented in the ear canal, at frequencies that are linear combination of the primary frequencies. Due to the cubic nature of the cochlear amplifier nonlinearity, the strongest DPOAE is observed at the frequency $f_{DP} = 2f_1 - f_2$. The level of this DPOAE is an objective and frequency-specific indicator of the cochlear functionality. Two mechanisms are assumed to contribute to the DPOAE: nonlinear generation of a backward and of a forward wave at the DP frequency in the cochlear region that is simultaneously excited at both primary frequencies, and linear reflection of the nonlinearly generated forward DP wave at its resonant cochlear place [15]. Both backward wave propagate along the BM and through the middle ear, and their vector sum is measured as a DPOAE in the ear canal.

In this work, we study a fast and reliable hybrid direct/multi iterative algorithm for solving the discretized counterpart of variations of nonlinear and nonlocal models proposed in [13] and in [16] built on the basis of the model proposed in [11] with the state-space formulation in the style of Elliott et al. [7].

In Section 2 we discuss two nonlinear nonlocal full cochlear continuous mod-

els and in Section 3 the underlying continuous models are converted into sequences of discrete problems. In Section 4 we analyze some issues of the approximate solution of the discrete models in Section 3 with special emphasis on the iterative solution of the sequences of large linear systems arising in the time-step process. In Section 5 we compare the typical behavior of the timings for two different approaches used to solve the underlying large scale linear systems for a distortion product example with the theoretical computational cost and the influences of the parameters of the experiments. Finally, in Section 6 we resume the results.

2. Nonlinear nonlocal full cochlear models

The cochlea contains the BM, that is immersed in an incompressible Stokes fluid. We concentrate on the upper cochlear chamber by simplifying it into a two dimensional rectangle $[0, L] \times [0, H]$, with the BM at $z = 0$. Signals generate vibrations on the left boundary at $x = 0$ at *stapes* level, which induce fluid motion that goes from the upper chamber to the lower chamber through the *helicotrema*, a small hole at $x = L$. Pressure gradients move the BM; see Figure 1. Symmetry allows to ignore details of helicotrema and to concentrate on the upper chamber, as in [11].
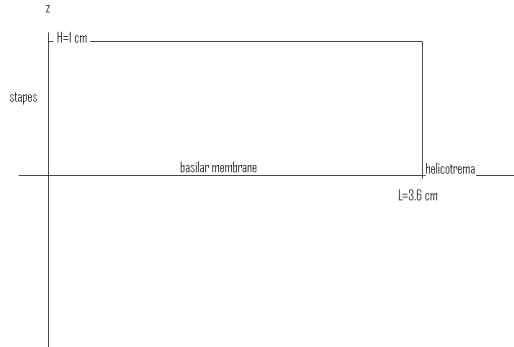

Figure 1: Simplified upper cochlear chamber: a two dimensional rectangle $[0, L] \times [0, H]$, with the BM at $z = 0$.

2.1. The continuous models

Let us summarize the model proposed in [13]. For an incompressible fluid, in a cochlear duct of rectangular constant cross section of constant half-height H and length L, divided by a tonotopically resonant elastic BM, the wave propagation along the cochlea on the BM, i.e., for $z = 0$, reduces to the one dimensional transmission line equation for the differential pressure p, which is

defined here as the difference between the pressure in the lower chamber and that in the upper chamber. With this sign convention a positive differential pressure drives a positive acceleration of the BM. The conservation of the momentum and of the mass of the fluid, which is assumed incompressible, implies:

$$\frac{\partial}{\partial x}p(x,0,t) = 2\rho\frac{\partial}{\partial t}V(x,0,t),\tag{1}$$

where V is the fluid longitudinal velocity, and the following relation between V and the BM transverse velocity at the longitudinal position x and time t:

$$\frac{\partial}{\partial x}V(x,0,t) = \frac{1}{H}\frac{\partial}{\partial t}u(x,t),\tag{2}$$

By deriving the first equation with respect to x and the second equation with respect to the time and combining the two, the propagation equation for the pressure is obtained:

$$\frac{\partial^2}{\partial x^2}p(x,0,t) = 2\frac{\rho}{H}\frac{\partial^2}{\partial t^2}u(x,t),\tag{3}$$

where ρ is the fluid density.

The following boundary condition also holds at the stapes:

$$\frac{\partial}{\partial x}p(0,z,t) = 2\rho\frac{\partial^2}{\partial t^2}u_{ow}, \quad 0 \le z \le H\tag{4}$$

where $\frac{\partial^2}{\partial t^2}u_{ow}$ is the acceleration of the stapes. Let us consider a uniform partition on the BM, $x = x_0, x_1, ..., x_N$, $x_i = i \cdot h$, $h = L/N$, where L is the length of the rectified cochlea. The term associated with the stimulus in the ear canal is a forcing term in the dynamical equation for the first element of the partition, i.e., $u_{ow}(t) = u(x_0,t)$ and, according to Talmadge et al. [19, eq. (10)],

$$\frac{\partial^2}{\partial t^2}u(x_0,t) + \gamma_{ow}\frac{\partial}{\partial t}u(x_0,t) + \omega_{ow}^2 u(x_0,t) = \frac{p(0,t) + G_{me}P_{dr}}{\sigma_{ow}}\tag{5}$$

where γ_{ow}, σ_{ow} and $K_{ow} = \omega_{ow}^2\sigma_{ow}$ are the phenomenological parameters chosen to represent the filtering properties of the middle ear, P_{dr} is the calibrated pressure in the ear canal (for a rigid ear drum), and G_{me} is the middle ear mechanical gain of the ossicles.

Considering the dynamical equation which relates the BM transversal displacement to the pressure p acting on the tonotopic oscillator, we have for the elements from 2 to $N-1$:

$$\frac{\partial^2}{\partial t^2}u(x,t) + \gamma_{BM}(x)\frac{\partial}{\partial t}u(x,t) + \omega_{BM}^2(x)u(x,t) = \frac{p(x,0,t) + q(x,t)}{\sigma_{bm}},\tag{6}$$

where q is the additional pressure given by the $OHCs$, γ_{BM} and ω_{BM}^2, damping and stiffness functions, respectively, are smooth functions of the x only in our setting. With some more computational efforts, dependency on the BM position

and velocity can be easily included. According to the Greenwood map, we set, as done in [13]:

$$\omega_{BM}(x) = \omega_1 + \omega_0\, e^{k_\omega x}, \quad \gamma_{BM}(x) = \gamma_1 + \gamma_0\, e^{k_\gamma x},$$

i.e., each tonotopic place is schematized by a single passive oscillator. An homogeneous Neumann boundary condition is assumed for pressure fluid field because the upper wall is rigid. The last element of the spatially discretized cochlea is the helicotrema, which is described, as usual, by a pressure release (short-circuit) boundary condition

$$p(L, z, t) = 0, \quad 0 \le z \le H. \tag{7}$$

The initial conditions are

$$u(x, 0) = 0, \quad \frac{\partial}{\partial t} u(x, 0) = 0, \quad 0 \le x \le L. \tag{8}$$

The *OHCs-BM* interaction can be schematized as a nonlinear, non-local active system. Active amplification and nonlinear saturation terms as additional forces triggered by the *OHCs* and acting on the *BM*, can be seen as generated by nonlocal *feed-forward* longitudinal interaction, similarly to what has been proposed by Kim and Xin [11], see also Bertaccini and Fanelli [2]. In particular, the force applied to the *BM* is transmitted to the *OHCs*, which act on the cilia and back on the *BM*. The pressure applied by *OHCs* on the *BM* is assumed proportional to the total pressure on the *BM*, and, due to the longitudinal tilt of *OHCs*, forces acting on the cilia at x cause *OHCs* to push at a point $x + \delta$ downstream on the *BM*

$$q(x + \delta, t) = \alpha(u, x, t) p_{BM} = \alpha(u, x, t)\,(p(x, t) + q(x, t)) \tag{9}$$

where p_{BM} is the total pressure on the *BM* and $\alpha = \alpha(u, x, t)$ is a nonlinear non-local gain factor, which depends on the *BM* displacement u in a cochlear region around the considered position x. Here we assume that $\delta = K\Delta_x$, $K \ge 1$ integer.

The underlying continuous *feed-forward* model can be resumed as below

$$\begin{cases} \dfrac{\partial^2}{\partial x^2} p(x, 0, t) = 2\dfrac{\rho}{H}\dfrac{\partial^2}{\partial t^2} u(x, t), \\ \dfrac{p(x, 0, t) + q(x, t)}{\sigma_{bm}} = \dfrac{\partial^2}{\partial t^2} u + \gamma_{BM}\,\dfrac{\partial}{\partial t} u + \omega_{BM}^2\, u, & 0 \le x \le L, \\ q(x + K\Delta_x, t) = \alpha(x, u, t)\,(p(x, 0, t) + q(x, t))\,, & 0 \le x \le L - K\Delta_x, \\ q(x, t) = 0, & 0 \le x \le K\Delta_x, \end{cases} \tag{10}$$

including initial (8) and boundary conditions (4)–(7).

A fruitful from the physiological point of view modification of the *feed-forward* dynamics is based on evaluating the effects of an additional OHCs force acting as an antidamping and directly proportional to the basilar membrane transversal velocity

$$q(x, t) = -\alpha(x, u, t)\gamma_{BM}\,\frac{\partial}{\partial t} u \tag{11}$$

proposed in Sisto et al. [16]. We call this variant a *feed-diagonal* model.

For the gain function α we use a variant of the integral expression proposed by Kim and Xin in [11]:

$$\alpha(u, x, t) = \alpha_0 g(< u(x,t)^2 >) \tag{12}$$

where

$$< u(x,t)^2 > = \frac{1}{\sqrt{\lambda\pi}} \int_0^L \exp\left(-\frac{(x-x')^2}{\lambda}\right) (u(x',t)^2)\, dx' \tag{13}$$

where γ is a dimensionless parameter controlling the strength of the non-local terms, and $\sqrt{\lambda}$ is a characteristic length (a constant in a scale-invariant cochlea), representing the longitudinal range of the non-local interaction.

For the *feed-forward model*, we choose the following nonlinear gain function g:

$$g(< u(x,t)^2 >) = 1 - \tanh\left(\frac{< (u(x,t) - u_0)^2 >}{u_{nl}^2}\right),$$

where u_{nl} is the OHC gain saturation, which approximately matches the nonlinear gain function by Kim and Xin [11] and by Lim and Steele [12], where u_{nl} is a transverse *BM* displacement scale for the nonlinear saturation of the *OHCs* gain, and u_0 is a parameter controlling the vertical asymmetry of the *OHCs* gain (in our setting $u_{nl} = 10^{-8}m$ and $u_0 = 0$).

More discussions on these models can be found in [13] and in [16].

The inclusion of a more complete description of the physiology would increase the computational complexity of the numerical solution of the problem. On the other hand, our approach seems to reproduce results in good agreement with the cochlear physiology.

3. The semidiscrete and discrete models

Unfortunately, a particular solution of the model (10) that can be useful for simulations, cannot be generated by analytical methods. We produce first a *semidiscrete* approximation of (10) with (4)–(7), i.e., another model that is still continuous in time but without partial derivatives with respect to the space variables, usually a sequence of systems of differential equations. Therefore, we get a fully discrete problem by providing time step integration for the semidiscrete one.

Semidiscretization, i.e. the process of discretization of partial derivatives with respect to the space only in an evolutionary partial differential equation can be found, e.g., in [10].

3.1. The semidiscrete models

In the style of [13], we divide the cochlea in N partitions of length Δ_x regarding each partition as a single oscillator with active amplification and nonlinear saturation terms as additional forces. Therefore, by discretizing with respect to

the space variable x, the coordinate on the cochlea, we get a system of $N+2$ differential equations, where N is the number of partitions on the rectified cochlea. Then, we use a time-step integrator to advance in time on an adaptive mesh.

By denoting with

$$P(t) = [p(x_1, 0, t) \ p(x_2, 0, t) \ ... \ p(x_N, 0, t)]^T$$

the vector including pressure at each cochlear partition $[x_{j-1}, x_j]$, $j = 1, 2, ..., N$ and similarly for $Q(t)$,

$$\Xi''(t) = \frac{\partial^2}{\partial t^2}[u(x_1, t) \ u(x_2, t) \ ... \ u(x_N, t)]^T$$

the vector of the cochlear partition accelerations and with

$$F = \frac{H}{2\rho \, \Delta_x^2} \begin{pmatrix} -\frac{3\Delta_x}{2H} & 2\frac{\Delta_x}{H} & -\frac{\Delta_x}{2H} & & & & \\ 1 & -2 & 1 & & & & \\ \ddots & \ddots & \ddots & & & & \\ & & & & \ddots & \ddots & \ddots & \\ & & & & 1 & -2 & 1 \\ & & & & & & -2\rho\frac{\Delta_x^2}{H} \end{pmatrix}, \qquad (14)$$

a $(N+2) \times (N+2)$ constant matrix, from (3), and (4), (7) for the first and last equations, respectively, we get

$$F P(t) = \frac{\partial^2}{\partial t^2}\Xi(t), \qquad (15)$$

which is a second order discretization with respect to the space variable x of the continuous problem. A second order discretization of (3) for $\partial^2 p/\partial x^2$, i.e., with respect to x only, is given by using standard centered differences with step Δ_x. On the other hand, we can show that the Neumann boundary condition (4) needs a one-sided formula involving not only $p(x_1, 0, t)$ and $p(x_2, 0, t)$ but $p(x_3, 0, t)$ in order to fully get the properties:

- (15) is a second order discretization (with respect to the space variables) of (4);

- the right hand side of (15) is preserved (the expression (15) is used inside other formulas; see below);

- no fictitious points are necessary for this second order discretization.

We note that the discretizations with respect to the space variables of Neumann boundary condition (4) in [7] and [13] are of first order only, generating a globally first order discretization of the models. Finally, the matrix F in

(14) is still nonsingular and has a condition number[1] in the euclidean norm $\kappa_2(F) = ||F||_2\,||F^{-1}||_2$ that is very similar to the one of the matrix F generated by using first order approximations for the boundary condition, i.e., less than $3\Delta_x^2/2$; see Section 4.1 for more details.

In the style of [13], let us write the continuous model (10) in compact form by the matrices A_E, B_E, C_E used in [13] and recalled below.

$$A_E = \begin{pmatrix} A_1 & & & \\ & A_2 & & \\ & & \ddots & \\ & & & A_N \end{pmatrix}_{2N \times 2N}, \qquad (16)$$

$$A_1 = \begin{pmatrix} -\gamma_{ow} & -\omega_{ow}^2 \\ 1 & 0 \end{pmatrix}_{2\times 2}, \quad A_i = \begin{pmatrix} -\gamma_{bm} & -\omega_{bm}^2 \\ 1 & 0 \end{pmatrix}_{2\times 2}, \; i = 2, ..., N-1$$

while A_N is a 2×2 null matrix; B_E and C_E are $2N \times N$ and $N \times 2N$ block diagonal matrices whose i-th blocks are

$$B_i = \begin{pmatrix} 1/\sigma_{bm} \\ 0 \end{pmatrix}, \quad C_i \begin{pmatrix} 1 & 0 \end{pmatrix}, \; i = 2, ..., N-1, \quad B_1 = \begin{pmatrix} 1/\sigma_{ow} \\ 0 \end{pmatrix},$$

respectively, and $A_N = 0$, $B_N = 0$. A matrix D_E was also defined which is the same of matrix C_E but with the poition of 0 and 1 inverted so that it could pick up the velocity component in the state space vector and which is also proportional to the passive damping term:

$$DE_i = \gamma_{bm} \begin{pmatrix} 0 & 1 \end{pmatrix}, \; i = 2, ..., N-1,$$

From (5)-(6) and the expression of A_E, B_E and C_E we can write

$$\frac{\partial}{\partial t} U(t) = A_E\,U(t) + B_E\,(P(t) + Q(t) + S(t)) \qquad (17)$$

$$\frac{\partial}{\partial t} \Xi(t) = C_E\,U(t), \qquad (18)$$

where $S(t)$ is a $2N$ vector whose only nonzero component is the first one: $C_{me}P_{dr}(t)$.

The feed-forward semidiscrete model

For the *feed-forward model* in [13], the expression of vector function $Q(t)$ can be deduced from the system

$$B(u,t)Q(t) = C(u,t)\,P(t), \qquad (19)$$

---

[1]We recall that the condition number $\kappa(T)$ of a matrix T is a measure of the sensitivity to the perturbations during the solution of linear systems $Tx = b$; see, e.g., [8] for more details.

a compact form of the third expression in (10), where B and C are $N \times N$ matrix functions defined as in [2] as lower bidiagonal matrices. In particular, B has ones and C has zeros on the main diagonal, respectively, and

$$B(i+K, i) = -\alpha(x_i, u, t), \quad C(i+K, i) = \alpha(x_i, u, t), \quad i = 2, ..., N-K, \quad (20)$$

i.e., $B = I - C$. Therefore, (19) can be uniquely solved.

By solving (15) with respect to $P(t)$ and inserting in (17) together with the expression of the vector function $Q(t)$ from (19) and again (15), we get the approximation of the continuous model with the infinite sequence of initial value problems, each one parametrized by Δ_x

$$\left(I - B_E(I + B^{-1}C)\, F^{-1}\, C_E)\right) \frac{\partial}{\partial t} U(t) = A_E U(t) + B_E\, S(t), \ U(0) \text{ assigned} \tag{21}$$

where the second derivatives of Ξ is substituted by differentiating (18). The mass matrices $M_{feed-forward}$ of the sequence (21) are not constant, non linear and nonlocal by the presence of the gain factor α in the entries of matrices B and C:

$$M_{feed-forward} = I - B_E(I + B^{-1}C)\, F^{-1}\, C_E = I - B_E\, B^{-1}\, F^{-1}\, C_E \tag{22}$$

while the Jacobian matrices of the initial value problems (21) are all equal to

$$J = A_E \tag{23}$$

and are constant.

The feed-diagonal semidiscrete model

Analogously, for the feed-*diagonal* model considered in [16] (i.e., such that (11) holds), we get the following expression for the mass matrix

$$M_{diagonal} = I - B_E\, F^{-1}\, C_E - B_E\, D\, D_E, \tag{24}$$

where D is a diagonal matrix such that

$$D(i, i) = \alpha(x_i, u, t), \quad i = 1, ..., N.$$

From here on, the pedices to the mass matrices will be neglected and the model used will be clear from the context.

3.2. The discrete model and time-step integration

The initial value problems (21) are *stiff* (see [9]) but are not *differential algebraic equations*, or *DAE* for short (see [9] for a definition) with the parameter chosen in [7], [13] and here, i.e., the mass matrix M (22) or (24) is not singular. In particular, for the *feed-forward* model (9), (10), the Jacobian J (23) and the transfer matrices

$$M^{-1} \cdot J \tag{25}$$

have eigenvalues with negative real parts spread in the interval $[-2.5 \cdot 10^3, -\mu]$ with $\mu > 0$ and imaginary parts varying in absolute value from 0 to more than 10^5; see Figures 2 and 3. Therefore, the semidiscrete model (21) reflects the behavior of the continuous one. No unstable modes are present. The presence of eigenvalues with large imaginary parts for the Jacobian and the transfer matrices suggests that the discretization in time requires small time steps and adaptivity with respect to the time discretization; see Section 5. The use of packages for time step integration with a finite region of stability, like one based on explicit formulas, are not appropriate here because

- the presence of a nontrivial mass matrix, changing at each step, suggests to avoid the transformation in a problem with the mass matrix equal to the identity as explicit time-step integrators do;

- the problem is *stiff* and the *stiffness* increases as the maximum value of the gain function α increases, provided it is less than one, otherwise the nature of the problem can change and other phenomena can take place (see Section 4.1) similarly to what observed in [2], even if the model considered in the latter research is different.
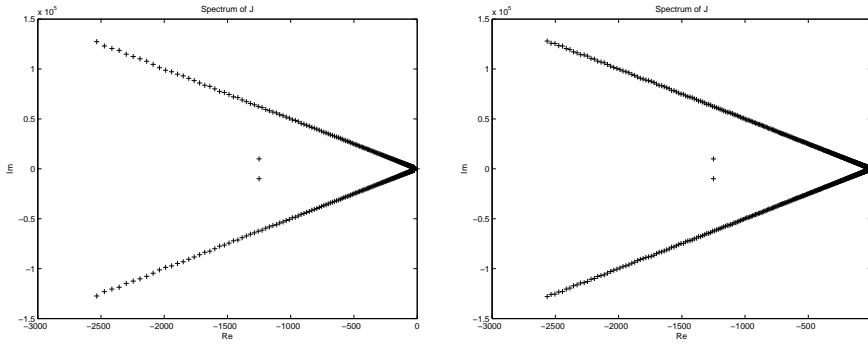

Figure 2: Typical behavior of the eigenvalues for the Jacobian matrix (23) J for $N = 200$ and $N = 400$, feed-forward model.

Time-step integration of the underlying semidiscrete systems (21) is performed here by modifying the code using iterative linear algebraic solvers proposed in [4] based on Mathworks' Matlab ® Ode15s package. We recall that ode15s is a variable-step, variable-order (here the maximum order is kept limited to 2) solver based on backward differentiation formulas (BDF) and other with similar properties (we force the use of BDFs for our simulations), implicit schemes based on *linear multistep formulas* which have an infinite region of absolute stability. For more on the nature of the formulas used in the package, the error estimation strategy for adaptive stepsize and the solution of the algebraic nonlinear equations see [17]. See [4] for another version of Ode15s with an iterative solver for
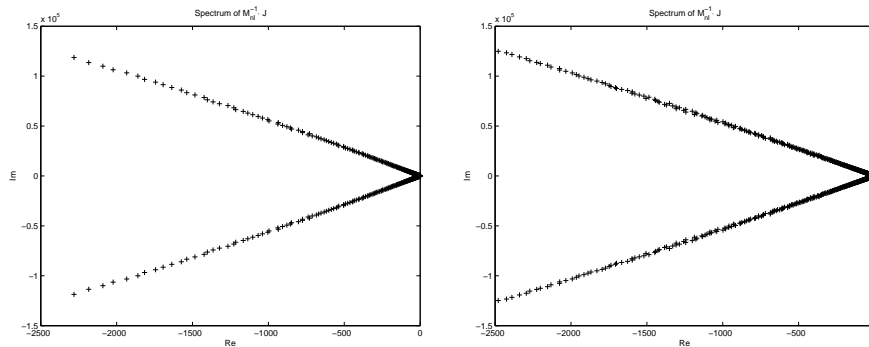
Figure 3: Typical behavior of the eigenvalues for the "transfer" matrix $Mass^{-1}J$ for $N = 200$ and $N = 400$, feed-forward model.

the algebraic linear systems applied to a 3D nonlinear reaction-diffusion model but where the mass matrix is trivial.

4. A multistage solver for the large scale algebraic systems

Time step integrators based on implicit linear multistep formulas require, at each integration step, the solution of algebraic nonlinear systems that are usually solved by *quasi-Newton* algorithms. The latters require to solve linear systems whose matrices can be written as

$$\mathcal{M}v = b, \quad \mathcal{M} = (M - a\,\Delta_t\,J), \tag{26}$$

where a is a constant and Δ_t is the time step. We stress that most of the overall computing time is spent on the solution of linear systems such as (26). This is a crucial issue for reliable and fast simulation. In particular, as observed in [13], the mass matrix, and therefore $\mathcal{M}$, is full, i.e., all of its entries are different from zero (and therefore the underlying differential equations are fully coupled) because B^{-1}, F^{-1} in (22) are full matrices even if B and F are banded, with nonzero entries in few diagonals only. On the other hand, iterative Krylov subspace solver like GMRES or BiCGstab (see, e.g., [14]) do not require to form matrix $\mathcal{M}$ explicitly to solve (26). They just need to perform matrix to vector products of the form $\mathcal{M} \cdot v$. This aspect is crucial in order to avoid inversion of matrices B and F, which is computationally expensive and unfeasible if N is large. We stress that F is constant but, in the *feed-forward* model, there is a component in the mass matrix, B^{-1}, that changes at each step because depends on α (and therefore on $u(t)$) and the matrix inversion costs $O(N^3)$ flops. A similar argument can be applied for other models whenever the feedback matrix B is not diagonal. On the other hand, in the *feed-diagonal* model(s), the matrix D in (24) is updated at each step but it is diagonal, therefore the cost of the inversion at each step is linear with N. Performing matrix-vector

products with the matrix $\mathcal{M}$ require the solution of two auxiliary linear systems with narrow band matrices. The structure of B and F and the fact that the considered models are one dimensional in space suggest the use of band-Gaussian elimination (see, e.g., [8]) because it is a direct method and, in this case, its cost is optimal (linear in the dimension of the rows of the matrices).

In order to let our "implicit" decoupling of the differential systems (17) be reliable, we need to consider the following issues:

- character of the mass and of the transfer matrices $M^{-1}J$;

- invertibility and conditioning of matrices B and F;

- convergence of iterations of the Krylov subspace solver;

- preconditioning the Krylov subspace solver.

The first issue is discussed in Section 3.2, the others below.

4.1. Conditioning of matrices B and F

The expression of the mass matrix (22) of the initial value problem (21) includes the inverses of the square matrices B as in (20) and both (22), (24) include the matrix F (14). Therefore, invertibility and conditioning of B and F are crucial in order to generate efficient and reliable simulations of (10) by the semidiscrete models (21). We recall that the former is a function of the BM displacement while the latter is constant. Despite this, as suggested in previous section, inversion and storage of F^{-1} should be avoided whenever N is large.

The matrix B. For what concerns matrix B, we observe that the lower bound on the condition number of B in [2, Proposition 1] is of no use here. In particular, the model studied in [2] uses in principle the same matrix function B as in (20), but with a different function α (see [2, formula (21)]), and while in [2] α can be greater than one, here the values of the gain factor α are always less than 1. This provide a well conditioned matrix.

Proposition 1. *Let us assume that $\alpha_{\max} = \max\{\alpha\} < 1$, where $\alpha = \alpha(x_s, u, t)$ is the gain factor defined as in (13). Therefore, the matrix B is well conditioned and its condition number can be bounded independently from the number of the mesh points on the basilar membrane,*

$$\kappa(B) = ||B|| \, ||B^{-1}|| < \frac{1 + \alpha_{\max}}{1 - \alpha_{\max}}.$$

Proof.

In order to give an upper bound for $||B^{-1}||$, we recall that the columns of B^{-1}, $c^{(k)}$, $k = 1, 2, ..., N$, are the solutions of the linear systems

$$B \, c^{(k)} = e^{(k)}, \quad k = 1, 2, ..., N,$$

where N is the number of rows of B and $e^{(k)}$ is the k-th unit vector of $\mathbb{R}^n$. By using an induction argument, if the jth entry of the kth column of B^{-1} is denoted by $c_j^{(k)}$, we get that

$$c_j^{(k)} = \prod_{s=1+k}^{j} \alpha(x_s, u, t), \quad k = 1, ..., N, \quad j = 1, ..., N,$$

with the convention that $\prod_s \emptyset = 1$. Therefore, by

$$||B^{-1}||_\infty = 1 + \sum_{r=0}^{N-3} \left(\prod_{s=2+r}^{N} \alpha(x_s, u, t) \right) \le 1 + \sum_{r=0}^{N-3} \left(\prod_{s=2+r}^{N} \alpha_{\max} \right)$$

and by recalling that $|\alpha_{\max}| < 1$, we get

$$||B^{-1}||_\infty \le 1 + \sum_{r=1}^{N-1} \alpha_{\max}^r = \sum_{r=0}^{N-1} \alpha_{\max}^r = \frac{1 - \alpha_{\max}^N}{1 - \alpha_{\max}} < \frac{1}{1 - \alpha_{\max}},$$

and therefore, by observing that $||B||_\infty = 1 + \alpha_{\max}$, we get

$$\kappa_\infty(B) < \frac{1 + \alpha_{\max}}{1 - \alpha_{\max}}.$$

$\square$

As predicted by the bound, the condition number of the matrix B is of the order of 2 both in the Euclidean and in the infinity norm whenever $\max\{\alpha\} = 0.36$, as is the case of normal hearing.

On the other hand, the proposed techniques can work even if $\max\{\alpha\} > 1$. In this case, B can be severely ill-conditioned, as observed in [2, Proposition 1].

The matrix F. Matrix F as in (14) connects the discrete versions of the differential pressure and cochlear partition acceleration; see equation (15). An analysis of its spectral properties is more difficult with respect to the first-order version of F of the model proposed in [7], the latter can be easily proved nonsingular by using Gerschgorin's Theorems; see, e.g., [18, Chapter IV]. The localization technique based on the field of values is not useful here as well because the symmetric part of F, i.e., $(F + F^T)/2$, is indefinite. By using the difference equation approach proposed in [3], we get that matrix F as in (14) is nonsingular and its eigenvalues are in the right half plane. Moreover, the condition numbers of F in the Euclidean norm are very much the same with respect of those of the matrix F in [7] and in [13]; see Table 1. We note that $\kappa_2(F)$ increases slightly more (by a factor of less than $3/2$) with N with respect to the condition number of the corresponding Toeplitz matrix $\tilde{F}$ resulting from F by removing its first and last rows. We recall that the condition number in the Euclidean norm for $\tilde{F}$ is $O(\Delta_x^{-2})$, Δ_x the mesh width on the rectified cochlea. Indeed, $\tilde{F}$ is the usual second order centered difference discretization of the one dimensional Laplacian operator; see, e.g., [10].

N	$\kappa_2(F)$	$\lambda_{\min}(F)$	$\lambda_{\max}(F)$
100	$3 \cdot 10^4$	-61.7	$-3.05 \cdot 10^{-3}$
200	$1.6 \cdot 10^5$	-247.1	$-3.08 \cdot 10^{-3}$
400	$8.4 \cdot 10^5$	-988.4	$-3.09 \cdot 10^{-3}$
800	$4.6 \cdot 10^6$	-3953.8	$-3.10 \cdot 10^{-3}$

Table 1: Condition number and minimum and maximum eigenvalues of matrix F.

4.2. Convergence of iterations of the Krylov subspace solver

As expected by the clustered (with respect to the mesh width parameter (Δ_x)) spectra observed for the matrices $\mathcal{M}$ in Figure 4, we experience a fast convergence of the Krylov subspace iterative solver GMRES solving the linear systems (26) for both the feed-forward and the feed-diagonal models; see Tables 2 and 3. It is interesting to see that these values are almost insensitive with respect to variations of the OHC gain parameter γ in (13) and thus with α. On the other hand, the matrix $\mathcal{M}$ of the algebraic linear systems arising at each step of the time-step integrator is nonsymmetric. Therefore, to predict the convergence behavior of the iterative solver used for the linear systems (26) necessary for the quasi Newton update step, we need in principle to know more information such as departure from symmetry or the condition number of the matrix of eigenvectors, the pseudospectra, etc; see, e.g., the convergence analysis of GMRES in [14] and the comments in [5, 6]. On the other hand, in our numerical tests, we found that very often eigenvalues can give realistic insights for the underlying nonsymmetric problem. In view of this, we will not consider this issue any further here.
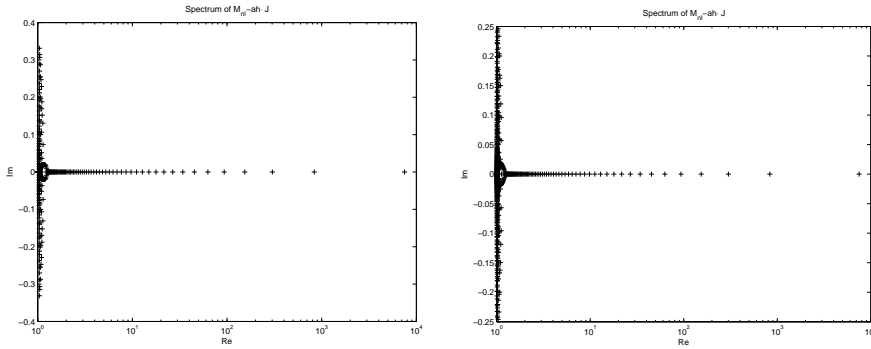
Figure 4: Typical behavior of the eigenvalues for iteration matrices $Mass - ahJ$ for $N = 200$ and $N = 400$.

4.3. Preconditioning the Krylov subspace solver

Whenever N, the number of grid points on the basilar membrane is reasonably large enough, we suggest iterative solution of algebraic linear systems

N	avg iters	total iters	factorizations
100	42	86756	135
200	46	100915	383
400	47	109104	649
800	48	115787	427
1600	47	115361	499

Table 2: Average and total number of iterations (for the iterative Krylov subspace solver) and number of LU factorizations (for the direct solver) of the matrix $\mathcal{M}$ (26), **feed-forward model**, $\gamma = 0.36$, stimulus: distortion product of two frequencies f_1 and f_2, $f_1 = 2\,Khz$ and $f_2 = 2.44\,Khz$, $\gamma = 0.36$, $Q_f = 5$.

N	avg iters	total iters	factorizations
100	42	87695	535
200	46	100954	607
400	47	110132	520
800	47	115333	575
1600	47	116088	538
3200	47	125454	601

Table 3: Average and total number of iterations (for the iterative Krylov subspace solver) and number of LU factorizations (for the direct solver) of the matrix $\mathcal{M}$ (26), **feed-diagonal model**, $\gamma = 0.36$, stimulus: distortion product of two frequencies f_1 and f_2, $f_1 = 2\,Khz$ and $f_2 = 2.44\,Khz$, $\gamma = 0.36$, $Q_f = 5$.

with matrices (26). With both the feed-forward and the feed-diagonal models considered here and the parameters in Section 5.1, we observe that the number of GMRES iterations are of the order of $42 \div 48$ and preconditioning strategies based, e.g., on incomplete factorizations produce an additional computational cost that is not compensated by a substantial reduction of the number of linear iterations. On the other hand, we do not exclude that future generalizations of the underlying models require a greater number of iterations for the convergence of the iterative part of the proposed hybrid iterative/direct strategy. In this case, a possible preconditioner for the feed-forward model can be based, e.g., on the following *constant* approximation of the matrix $\mathcal{M}$ as in (26):

$$ P = (I - B_E\, F^{-1} C_E) - a\, \tilde{h}\, J, $$

i.e., the matrix $G(U)$ is approximated by the identity (or by another constant matrix) and $\tilde{h}$ is an average of the typical step sizes used by the time-step integrator. In order to avoid working with a *full* preconditioner (because F^{-1} is a full matrix), we need to apply P implicitly. In particular, we recall that the matrix P can act through matrix-vector product only because of the use of the Krylov subspace solver. Therefore, the application of the (left) preconditioner operator P for the matrix vector product $w = \mathcal{M}v$, i.e. $w = P^{-1}\mathcal{M}v$ required by GMRES algorithm, can be realized with the mathematically equivalent two steps: (1) compute $\tilde{w} = \mathcal{M}v$; (2) solve the linear system $Pw = \tilde{w}$ for w.

A more accurate preconditioner should approximate step by step the matrix $\mathcal{M}$ that changes with h and U. In order to avoid recomputing a new approximation operator from scratch at each step, we suggest the use of the updating strategy for preconditioners proposed in [1].

5. Simulations and performances

In this section we report some numerical experiments with the proposed packages. All tests were performed on a Intel®Core^{TM}2 Duo Mobile Processor T9550 2.66 Ghz clock L2 Cache Size 6Mb, L2 Cache Speed 2.66 GHz, bus speed 1066 MHz, 4Gb Ram running Linux Fedora 12/64 bit running Matlab R2009a 64 bit. The second core is enabled during test sessions devoted to report timings but its contribution to the computation is negligible.

5.1. The parameters.

The main parameters we consider are mostly the same of those in [13] and in [16].

L	$3.5 \cdot 10^{-2}\,m$	Length of the cochlea
H	$10 \cdot 10^{-3}\,m$	Height of the cochlea
N	$500 \div 20000$	Number of cochlea discrete partitions
ρ	$10^3\,kg\,m^{-3}$	Fluid density
k_0	$3.1 \cdot 10^3\,m^{-1}$	Cochlear geometrical wavenumber
ω_0	$2.08 \cdot 10^4 \cdot 2\pi\,s^{-1}$	Greenwood's map frequency coefficient
ω_1	$-145 \cdot 2\pi\,s^{-1}$	Greenwood map's frequency offset
σ_{BM}	$5.5 \cdot 10^{-2}\,kg\,m^{-2}$	BM density
k_ω	$1.382 \cdot 10^2\,m^{-1}$	Greenwood map's inverse length scale
γ_0	$5.035 \cdot 10^3\,s^{-1}$	Cochlear damping map coefficient
γ_1	$100\,s^{-1}$	Cochlear damping map offset
k_Γ	$1.382 \cdot 10^2\,m^{-1}$	Cochlear damping map inverse length scale
K_{ow}	$2 \cdot 10^8\,N\,m^{-3}$	Effective middle ear-oval window stiffness
γ_{ow}	$5 \cdot 10^3\,s^{-1}$	Effective middle ear-oval window damping
σ_{ow}	$2\,Kg\,m^{-2}$	Effective middle ear-oval window density
u_{nl}	$10^{-8}\,m$	BM displacement saturation length scale
γ	0.36	OHC gain parameter
λ	$3.4641 \cdot 10^{-4}\,m^2$	OHC nonlocal interaction range

5.2. The numerical results

In the sequel, we show a comparison of the timings for both the feed-diagonal and the feed-forward models with an input based on two primary tones $f_1 = 2000\,Hz$ and $f_2 = 2440\,Hz$, whose level differ by $10\,dB$ with the level of f_2 equal to $60\,dB\,SPL$, where SPL means sound pressure level. This kind of input generates the so called *distortion product* at the frequency $f_{DP} = 2f_1 - f_2$. The spectral line corresponding to this distortion product, along with the others at frequencies that are different linear combinations of the primary frequencies, may be observed in the spectrum of the cochlear response estimated at the stapes (the first partition of the model) in Figure 5.

We compare the standard direct and our hybrid iterative/direct solution of the linear system of the quasi Newton correction step in the Matlab package for time-step integration ode15s. Global timings (see Figures 6 and 7) show that there is a tradeoff mesh size in space, i.e., there exist $\overline{\Delta_x}$ and $\overline{N}$ such that, for $\Delta_x \le \overline{\Delta_x}$ or, equivalently, for $N \ge \overline{N}$, the hybrid iterative/direct strategy proposed in Section 4 is computationally more convenient with respect to our implementation of the direct solution of linear systems as in (26). From the tradeoff point on, as the mesh get refined, the performance of the underlying iterative solution get greater. Moreover, there exists also a sort of "cut-off point" dependent on the machine main memory, i.e., beyond this point, the direct solution of the semidiscretized model cannot be performed at all without resorting to the disk swap memory space, which is typically slower with a factor of $1000 - 10000$ with respect to the RAM and the timings increase unacceptably for a reasonable use of the simulation (e.g., days instead of minutes). We note that the tradeoff point is different for the two variants of the active cochlear model considered here. In particular, even if the semi discrete system of differential equations (17) is still fully coupled for all models, the feed-diagonal
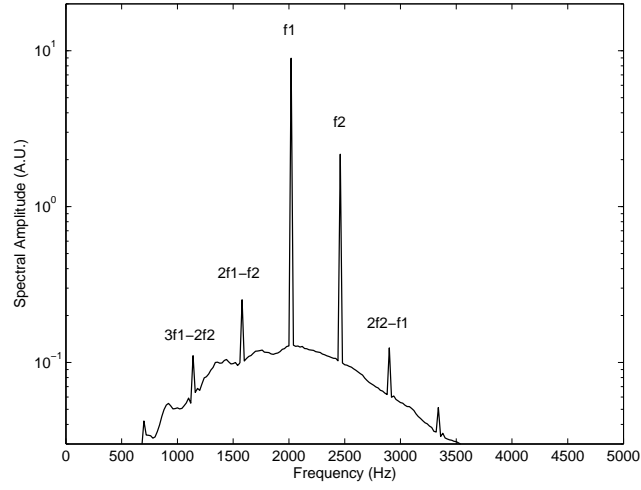
Figure 5: DPOAE response at the stapes. The two primary lines are surrounded by several DP lines, the strongest being that of frequency f_{DP}.
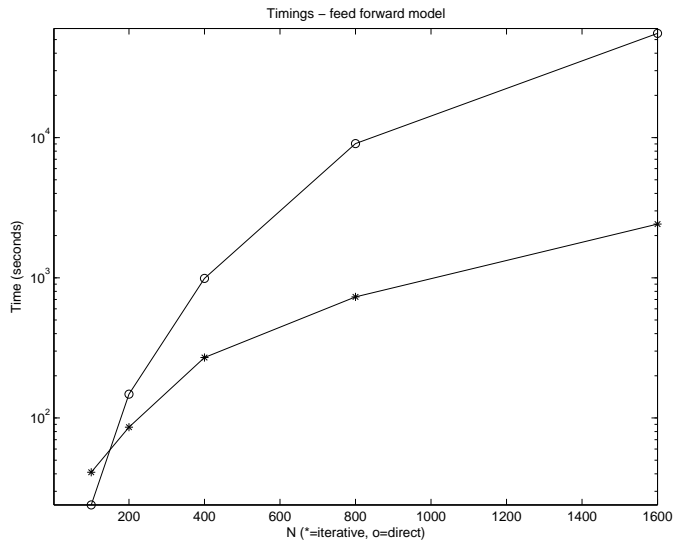

Figure 6: Comparison of timings for the feed-forward model. The circles and stars stand for the direct vs. hybrid-iterative solution of the large scale system (26), respectively.

model does not require a new $N \times N$ matrix inversion at each time step as the feed-forward does by using a direct solver for (26). Therefore, as expected,
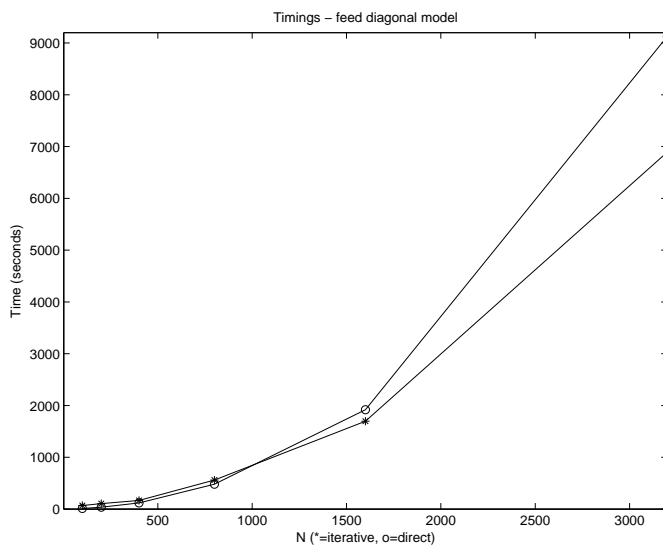
Figure 7: Comparison of timings for the feed diagonal model. The circles and stars stand for the direct vs. hybrid-iterative solution of the large scale system (26), respectively.

we observe that the advantages of our hybrid iterative/direct strategy over our implementation of the direct solution of (26) by using Gaussian elimination is much greater for the feed-forward model. Similar results would be observed for, e.g., a feed-backward model and other variants using a non diagonal feedback matrix.

We conclude by observing that, in order to get a simulation from zero to 20 milliseconds with stimuli from $2Khz$ to $3Khz$, a relative error tolerance of 10^{-3} requires a time step from $5 \cdot 10^{-6}$ to 10^{-5}, thus generating approximately from 3000 to 4000 steps. Of course, different stimuli can show different computational costs, but the distortion product is a good benchmark with respect to simpler stimuli such as the click or the single exponentially decaying sinusoid. On the other hand, timings are almost insensitive to changes of parameters such as the OHC gain factor γ, and thus on α, provided $\alpha < 1$.

We verify the convergence of the proposed scheme by checking ratios

$$||u_N - u_{2N}||/||u_{2N} - u_{4N}||_2$$

finding that the scheme is globally of second order. We recall that the discretization with respect to the space variable is of order two while with respect to time is up to order five.

6. Conclusions

A full second order time-step package for some recently proposed nonlinear, nonlocal models for inner ear is considered here. An analysis of the discrete

counterparts of a feed-forward and of a feed-diagonal models were performed. The convergence of an hybrid iterative/direct solver for the large scale algebraic linear systems generated by the discretization of the underlying models was studied in view of the parameters of the continuous model, founding that conditioning and timings are relatively insensitive to changes of the gain factor parameters. On the other hand, we observed that the implicit decoupling realized by our hybrid solver for the semidiscretized model is essential in order to provide a computational cost within $O(N)$ and $O(NlogN)$, N the number of mesh subdivisions on the rectified cochlea, instead of $O(N^3)$.

The guidelines proposed here can be used for other variant of full active cochlear models in the style of those proposed in [7, 13, 16]. In particular, we expect that multidimensional generalizations of the proposed nonlinear and nonlocal cochlear models will even more greatly benefit by the use of the proposed approaches.

[1] S. Bellavia, D. Bertaccini and B. Morini, Nonsymmetric preconditioner updates in Newton-Krylov methods for nonlinear systems, SIAM J. Sci. Comput. (2011), in press.

[2] D. Bertaccini, S. Fanelli, Computational and conditioning issues of a discrete model for sensorineural hypoacusia, Appl. Numer. Math. 59 (2009) 1989–2001.

[3] D. Bertaccini, F. Di Benedetto, Spectral analysis of nonsymmetric quasi-Toeplitz matrices with applications to preconditioned multistep formulas, SIAM J. Numer. Anal. 45–6 (2007) 2345–2367.

[4] D. Bertaccini, D. Calvetti, Fast simulation of solid tumors thermal ablation treatments with a 3D reaction diffusion model, J. Comp. Biol. Med. 37 (2007) 1173–1182.

[5] D. Bertaccini, G. H. Golub and S. Serra-Capizzano, Spectral analysis of a preconditioned iterative method for the convection-diffusion equation, SIAM J. Matr. Anal. Appl. 29 (2007) 260–278.

[6] D. Bertaccini and M. K. Ng, Band-Toeplitz preconditioned GMRES iterations for time-dependent PDEs, BIT 43 (2003) 901–914.

[7] S.J.Elliott, E.M. Ku, B. Lineton, A state space model for cochlear mechanics, J. Acoust. Soc. Am. 122 (2007) 2759–2771.

[8] G. H. Golub, C. Van Loan, Matrix Computations, third edition, John Hopkins University Press, Baltimore, London, 1996.

[9] J. D. Lambert, Numerical methods for ordinary differential systems, John Wiley & Sons, Chichester, 1991.

[10] R. J. LeVeque, Finite difference methods for ordinary and partial differential equations, SIAM, Philadelphia, 2007.

[11] Y. Kim, J. Xin, A two-dimensional nonlinear nonlocal feed-forward cochlear model and time domain computation of multitone interactions, Multiscale Model. Simul. 4-2 (2005) 664-690.

[12] K.M. Lim, C.R. Steele, A three dimensional nonlinear active cochlear model analized by the WKB-numeric method, Hearing Research, Vol. 170 (2002) 190–205, 2002.

[13] A. Moleti, N. Paternoster, D. Bertaccini, R. Sisto and F. Sanjust, Otoacoustic emissions in time-domain solutions of nonlinear non-local cochlear models, J. Acoust. Soc. Am. 126 (2009) 2425-2436.

[14] Y. Saad, Iterative Methods for Sparse Linear Systems, PWS publishing company, Boston, MA, 1995.

[15] C. A. Shera, J.J., Jr Guinan, Evoked otoacoustic emissions arise from two fundamentally different mechanisms: A taxonomy for mammalian OAEs, J. Acoust. Soc. Am. 105 (1999) 782–798.

[16] R. Sisto, A. Moleti, N. Paternoster, T. Botti and D. Bertaccini, Different models of the active cochlea, and how to implement them in the state-space formalism, J. Acoust. Soc. Am. 128 (2010) 1191–1202.

[17] L. F. Shampine, M. W. Reichelt, The MATLAB ODE Suite, *SIAM J. Sci. Comp.*, 18 (2007) 1–22.

[18] G.W. Stewart, J.G. Sun, Matrix perturbation theory, Academic Press, NY, 1990.

[19] C. L. Talmadge, A. Tubis, G. R. Long, P. Piskorski, Modeling otoacoustic emission and hearing threshold fine structures, J. Acoust. Soc. Am. 104 (1998) 1517-1543.